



## Experimental study of a stand-alone solar-wind-powered reverse osmosis seawater desalination system

Zhilong Xu, Judong Liu, Zhongming Huang, Xiaofan Yang, Su Wang, Fang Fang, Shuwang Chen, Yongqing Wang\*

*College of Mechanical and Energy Engineering, Jimei University, Xiamen 361021, China, Tel. +86 592 6180597; Fax: +86 592 6183523; emails: yongqing@jmu.edu.cn (Y. Wang), zhilong.xu@163.com (Z. Xu), liujd@jmu.edu.cn (J. Liu), hzm0513@163.com (Z. Huang), yangxf@jmu.edu.cn (X. Yang), 163swang@163.com (S. Wang), xqfangfang@tom.com (F. Fang), chenshuwang0530@163.com (S. Chen)*

Received 27 August 2016; Accepted 11 December 2016

### ABSTRACT

An experimental photovoltaic-wind-powered seawater desalination system with a design capacity of 1 m<sup>3</sup>/d was developed and tested in Xiamen, China. A 5-kWp photovoltaic array was used as the main driving source, and two 0.5-kW wind generators as the supplementary source. A small-capacity battery bank for 1.5 h of system autonomy was equipped, and an electricity equilibrium/buffer controller was specially developed to manage the produced, demanded, stored, and rejected power of the system. The desalination unit used was a three-stage reverse osmosis (RO) unit without energy recovery device. The system was operated in an automatic mode throughout September and October 2015, showing good suitability to unsteady solar and wind energy, during which the RO unit ran for 6.1 h/d averagely, showing reliable performance in the intermittent off-and-on operation mode. The daily water production ranged from 0 to 1.56 m<sup>3</sup>/d, and the daily average was 0.92 m<sup>3</sup>/d. Using real seawater with a salinity of 31,000 ppm as feed, the system obtained a salt retention rate over 99% and a water recovery ratio about 20%. The specific energy consumption of freshwater was 17 kWh/m<sup>3</sup>, with the ways to lower it discussed.

*Keywords:* Stand-alone desalination; Photovoltaics; Wind power; Reverse osmosis

### 1. Introduction

The combined effect of the continuous increase in the world population, the increase in per capita water demand caused by the change of life style, and the decrease in the availability of potable water resource caused by climate change and contamination makes water desalination an important way of providing sustainable source of freshwater for many arid areas in the world. The global capacity of commissioned desalination plants was over 86.8 million m<sup>3</sup>/d by June 30, 2015 [1]. Desalination is an energy-intensive industry, which not only depletes the fossil fuels that are typically used as the energy source but also causes emissions of greenhouse and other undesirable gases. In recent years, there has been an obvious interest in renewable-energy-powered

desalination systems [2,3], of which solar photovoltaic (PV) driven reverse osmosis (RO) desalination, solar still, wind-driven RO desalination, and solar thermal membrane distillation are the most representative.

It has been demonstrated that compared with solar-only and wind-only power generation systems, hybrid solar and wind systems have the potential to provide more reliable power sources in changing weather conditions [4], indicating more stable water production when being used to drive desalination processes. The combination of hybrid PV-wind power generation units, which are characterized by low maintenance requirements and short construction time [5], and RO units, which are characterized by relatively low energy consumption and cost [6], has attracted the attention of some researchers [5–17].

Koutroulis and Kolokotsa [6] proposed an optimal sizing method for minimizing the 20-year round total cost of

\* Corresponding author.

a PV-wind-RO system, with the results showing that the hybrid-powered systems were more profitable than the separate PV-powered and wind-powered systems. Mohamed and Papadakis [7] presented a simplified method for sizing and simulating PV-wind-RO systems, and the case study showed a calculated water cost of 5.2 €/m<sup>3</sup>. Cherif and Belhadj [8] proposed a system consisting of a 400-m<sup>2</sup> PV array, a 10-kW wind turbine, and a two-stage RO unit, and estimated the monthly energy and water production under climatic conditions of southern Tunisia. Mokheimer et al. [9] proposed an optimal sizing method for PV-wind-RO systems and optimized the system components under a constant RO load of 1 kW for operation time of 12 and 24 h/d, respectively, obtaining an energy consumption ranging between 8 and 20 kWh/m<sup>3</sup> and a water cost ranging between 3.693 and 3.812 \$/m<sup>3</sup>. Mousa et al. [10] optimally designed a small-size system and obtained a water cost of 0.498, 0.851 and 1.211 \$/m<sup>3</sup> when the specific energy consumption (SPC) of freshwater was 2.5, 5.0 and 7.5 kWh/m<sup>3</sup>, respectively. Kershman et al. [11] investigated a PV-wind-grid-RO system with a design water capacity of 300 m<sup>3</sup>/d and predicted that the levelized water cost would increase by not more than 45% compared with the grid-power-only solution. Using a pumped storage unit rather than traditional batteries as energy storage unit, Spyrou and Anagnostopoulos [12] investigated the optimal design of a hybrid-powered RO system and obtained a water cost range of 1.5–3 €/m<sup>3</sup>.

Besides the theoretical studies performed on PV-wind-RO systems mentioned above, a few experimental setups have been built, with the general information summarized in Table 1. All the established systems were off-grid small-scale systems, of capacity not more than 20 m<sup>3</sup>/d. Although there are several different energy storage alternatives like water pumping, flywheels, batteries, and hydrogen storage, batteries were used in all the experimental systems. The system reported in reference [16] had the longest running period, about 3 years, with a water cost of 12.6 ¥/m<sup>3</sup>, much higher than that of 5–6 ¥/m<sup>3</sup> [18] for the conventional grid-powered RO systems. The high capital cost of the PV and wind generators, especially the former, was the main reason for the high water cost [7]. Although unable to compete with the grid-powered RO systems economically so far, the autonomous, low-maintenance PV-wind-RO systems have a big advantage when used to produce desalinated water for remote and isolated areas lacking portable water and electrical grid.

The objective of the present work was to investigate experimentally the performance of a stand-alone hybrid PV-wind-powered RO seawater desalination system. The experimental setup was built in the city of Xiamen (24°23′–24°54′ N and 117°53′–118°26′ E [20]) in Fujian Province, a coastal province in the southeast of China. There are about 1,500 islands over 500 m<sup>2</sup> in Fujian [21], and most of them are far from the electrical grid. Considering the high cost of

Table 1  
General information of established hybrid PV-wind-RO desalination systems

Reference number	[13]	[14]	[5]	[15]	[16]	[17]
Geographic location	Heelat Ar Rakah, Oman	Israel	Attiki, Greece	Nanao, China	Dongshan, China	Zhejiang, China
Operation mode	Off-grid	Off-grid	Off-grid	Off-grid	Off-grid	Off-grid
Design water output	5 m <sup>3</sup> /d	3 m <sup>3</sup> /d	130 L/h	20 m <sup>3</sup> /d	20 m <sup>3</sup> /d	25 L/h
Feed salinity or TDS, ppm	1,010	4,000	37,000	29,100	N/A	N/A
Power of PV array, kWp	3.4 <sup>b</sup>	3.5	4	13.1	5	0.28
Number of PV panel	64	64	36	146	N/A	2
Tilt angle of PV array	40°	N/A	Two angles	28°	N/A	N/A
Rated wind power output, kW	10 <sup>c</sup>	0.6	0.9	33	15	1
Number of wind turbine	1	1	1	11	N/A	1
RO operation pressure, MPa	N/A <sup>a</sup>	1.4–1.6	5.8	5.5	N/A	5.0
Pressure recovery device	Not included	N/A	N/A	Not included	N/A	Included
Model of membrane element	N/A	N/A	SW30–2540 <sup>d</sup>	SW30–4040 <sup>d</sup>	N/A	SW30–2521 <sup>d</sup>
Number of membrane element	12	2	2	6	N/A	1
Water recovery ratio, %	70	50	15	30	N/A	7.5
Battery bank capacity, Ah	N/A	1,500	1,850	9,600	400	400
Freshwater salinity, ppm	34	200	230	<1,000	N/A	N/A
Running period	N/A	N/A	N/A	N/A	3 years	2 months
Specific power consumption of produced water, kWh/m <sup>3</sup>	N/A	N/A	N/A	N/A	10.9	4.8 <sup>e</sup>
Water cost	N/A	N/A	N/A	N/A	12.6 ¥/m <sup>3</sup>	N/A

<sup>a</sup>N/A = Not available.

<sup>b</sup>Value calculated from the reported data.

<sup>c</sup>Wind power was used to run a pump to abstract groundwater for both desalination and irrigation.

<sup>d</sup>Membrane produced by Dow Filmtec [19].

<sup>e</sup>The value is doubtful.

water shipping from the mainland, stand-alone PV-wind-powered desalination systems are under planning for several inhabited islands, and the one presented here is a small-scale experimental system with a design water capacity of 1 m<sup>3</sup>/d, from which we intend to improve the understanding of the system performance and get some experience in system design and operation.

## 2. Description of the experimental setup

Fig. 1 shows the schematic diagram of the experimental system, which mainly consists of a solar PV array, two wind generators, a storage battery bank, an electricity equilibrium/buffer controller, a direct current (DC)/alternative current (AC) inverter, and an RO desalination unit. The first five units are used to ensure a stable power input to the RO unit, among which the solar and wind generators are power production units; the battery bank is an energy storage (by charging) and compensation (by discharging) unit; the equilibrium/buffer controller is used to realize an effective energy management of the system; and the DC/AC inverter is used to convert DC to AC. The arrows in Fig. 1 indicate the direction of energy flows. A monitoring and control system (not shown in Fig. 1) is also included to monitor/record the operating parameters and realize automatic control of the experimental system.

### 2.1. RO desalination unit

The configuration of the RO desalination unit is schematically shown in Fig. 2. It consists of a feed pump, a pre-treatment unit, a high-pressure pump, an RO membrane

module, and a cleaning tank, with the instruments for pressure, conductivity, and flow rate measurement at locations shown in Fig. 2.

Driven by the feed pump, feed seawater is pretreated in a multi-media filter, a 5- $\mu$ m cartridge filter, and a 1- $\mu$ m cartridge filter sequentially, to remove the particles and ions harmful to RO membranes. In the high-pressure pump, the feed is pumped to a pressure high enough to overcome its osmotic pressure, and then introduced into the membrane module. To protect the membranes, a frequency converter was added to realize a variable-frequency start-up of the high-pressure pump. Three Filmtec [19] spiral-wound membrane elements (SW30–2540), each installed in one pressure vessel, were connected in series to be a three-stage module. The nominal water recovery of the membrane element is 8%, and the maximum operating pressure is 5.5 MPa. Routed into the first stage of the RO module, the feed seawater is separated into permeate and concentrate. The concentrate is used as the feed of the second stage where it is further concentrated and then used as the feed of the third stage. The permeate from the three stages is output as product water. The operating pressure of the membrane module can be regulated by changing the opening of the pressure-regulating valve installed in the outlet pipe of the membrane concentrate. To protect the membranes, a small amount of permeate is stored in the cleaning tank for membrane washing after operation every day.

A centrifugal pump (CHL4-30) with a motor power of 0.55 kW serves as the feed pump, and a piston pump (RS-SS15) with a motor power of 1.5 kW and maximum operating pressure of 10 MPa serves as the high-pressure pump.

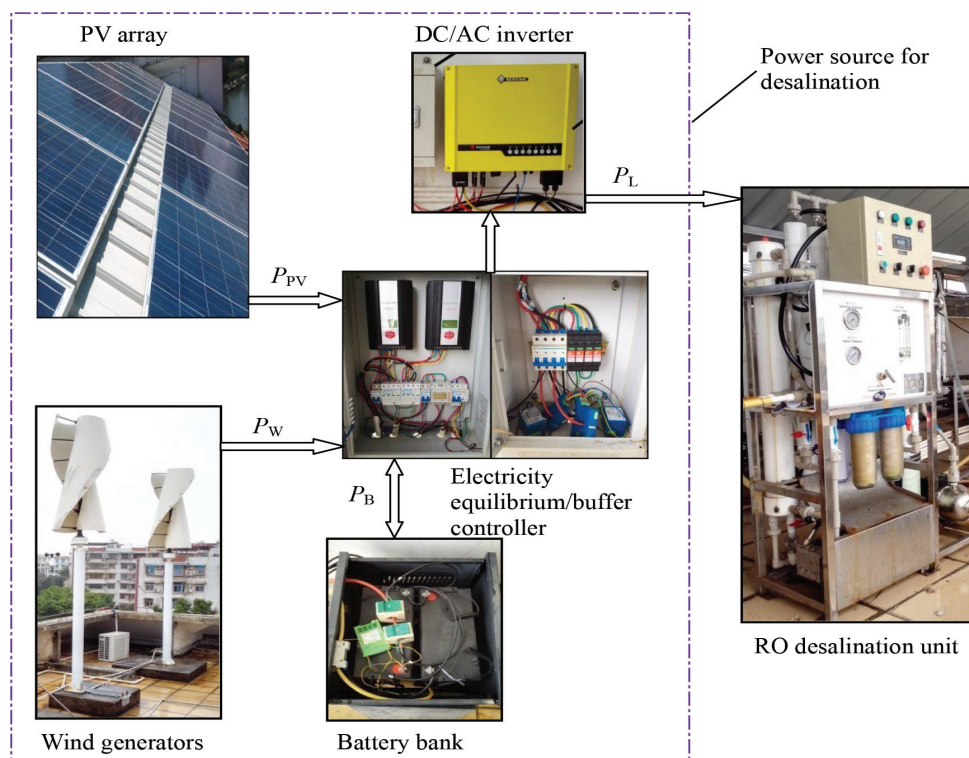


Fig. 1. Schematic diagram of the hybrid PV-wind-powered RO desalination system.

Both the pumps are run by 220 V AC. The electricity need of the pumps and the monitoring/control system was estimated to be 2.1 kW.

2.2. PV array

Table 2 shows the monthly average air temperature, solar insolation, and wind speed of Xiamen [22,23]. For a fixed-slope PV system as used in our experiments, a slope roughly equal to the local latitude usually leads to a maximum annual PV energy production [8], so the solar insolation on the south-facing surface tilted 24° to the horizontal

was calculated (Table 2). As a measure of wind power, the wind power density determined by wind speed and air density was also calculated (Table 2). With an annual average wind velocity of 3 m/s and annual average power density of 17.3 W/m<sup>2</sup>, the experimental site is not rich in wind resource, so in our design, solar energy was used as the main energy source, while wind energy as the supplementary source.

The annual electricity consumption of the system was estimated to be 5,400 kWh. The solar panel selected is 1,950 mm long, 992 mm wide, and 45 mm thick, with rated power of 250 Wp, rated voltage of 36 V, and rated current

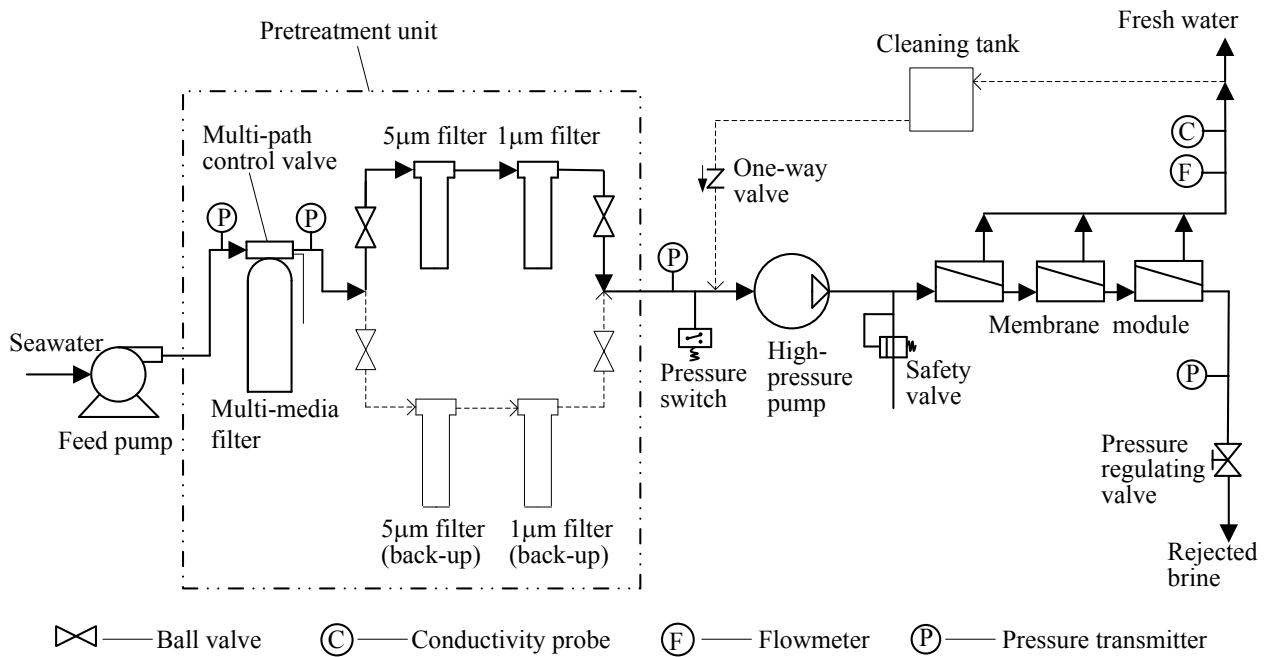


Fig. 2. Schematic diagram of the RO seawater desalination unit.

Table 2  
Climatic conditions of Xiamen, China [22,23]

Month	Ambient temperature (°C)	Solar insolation on horizontal surface (MJ/m <sup>2</sup> )	Solar insolation on 24° tilted surface (MJ/m <sup>2</sup> )	Wind speed (m/s)	Wind power density (W/m <sup>2</sup> )
January	12.5	285.7	377.1	3.11	18.54
February	12.4	221.4	247.9	3.16	19.46
March	14.6	299.4	332.3	2.97	15.75
April	18.7	343.3	384.5	2.70	11.65
May	22.6	440.5	493.4	2.65	10.81
June	25.8	437	489.2	2.95	14.73
July	27.8	529	640.1	2.91	13.97
August	27.6	499.5	609.4	2.81	12.66
September	26.0	468.8	571.9	3.07	16.62
October	23.0	415.9	544.8	3.61	27.71
November	19.2	349.7	461.6	3.43	24.21
December	14.6	324.6	431.7	3.25	20.92

of 6.95 A. The monthly electricity production of a single PV panel installed at a tilt angle of  $24^\circ$  was calculated (with the results shown in Fig. 3), amounting to an annual output of 272 kWh. Twenty panels, ten in series and two in parallel, were used to meet the energy need of the system.

### 2.3. Wind generators

The vertical-axis S500V1-48 wind generator with a rated power of 500 W and rated voltage of 48 V was chosen. The output power of wind generator depends on the wind speed at the hub height and the output characteristics of the generator. Based on the Weibull distribution model [24], the monthly probability density function of wind speed was calculated for Xiamen, and then, based on the performance curve of the S500V1-48 wind generator, the monthly electricity production was calculated, with the results shown in Fig. 4. Two wind generators were installed, with a total annual power of 1,200 kWh predicted.

### 2.4. Battery bank

Renewable-energy-powered RO systems usually contain a large battery bank to provide 2 or 3 d of operation autonomy [25]. The problem is that: (1) with a short life expectancy, the batteries are considered to be the most problematic part of the system, especially in remote areas where they are usually poorly maintained [26]; (2) considerable energy loss occurs in the charge/discharge cycle of the batteries [26]; and (3) the cost of large battery banks is high, for which one of the examples is from reference [7] where the annual cost of the batteries accounted for 12% of the total annual system cost.

To reduce the influence of battery-caused problems, a small-capacity battery bank with only 1.5 h of operation autonomy was used in our experimental system. Four OT100-12 lead acid batteries were connected in series, and the rated capacity and rated voltage were 400 Ah and 48 V, respectively.

### 2.5. Electricity equilibrium/buffer controller

An electricity equilibrium/buffer controller was specially designed to perform a round-the-clock electricity management of the system, with the principle shown in Fig. 5. It is composed of a calculation unit, high-frequency detection modules, feedback circuits, and a charge/discharge

protection unit of battery bank. The output power of PV and wind generators,  $P_{PV}$  and  $P_W$ ; the load demand,  $P_L$ ; the charge power,  $P_{ch}$  or discharge power,  $P_{dch}$ ; and the charge capacity of battery bank,  $Q_B$ , are detected at a frequency of 50 times/s, with the signals transmitted to the calculation unit through the feedback circuits. It should be noted that surplus power exists when  $P_{PV} + P_W > P_L + P_{dch}$ , so an energy rejection unit (ERU) is included where the surplus electrical energy is converted into heat energy through resistors.

Fig. 6 shows the energy management algorithm applied by the calculation unit. To protect the batteries, a high charge limit  $Q_{B(high)}$  and a low limit  $Q_{B(low)}$  95% and 10% of the full capacity, respectively, were set. In the case of  $P_L > 0$  (RO unit is under operation) and  $P_{PV} + P_W > P_L$ , part of the produced power is used to drive the RO unit and the monitoring/control system, and the balance is either rejected through ERU (when  $Q_B \cong Q_{B(high)}$ ), or used to charge the battery bank with the surplus (if any) introduced into ERU (when  $Q_B < Q_{B(high)}$ ). In the case of  $P_L > 0$  and  $P_{PV} + P_W < P_L$ , the battery bank discharges to make up the power shortage when  $Q_B > Q_{B(low)}$ , while the RO unit is shut down when  $Q_B \cong Q_{B(low)}$ . In the case that the RO unit is out of operation, the produced electricity is either rejected through ERU (when  $Q_B \cong Q_{B(high)}$ ), or used to charge the batteries with the surplus (if any) consumed in ERU (when  $Q_B < Q_{B(high)}$ ).

### 2.6. DC/AC inverter

A GW5048D-ES inverter was selected to convert DC to 220 V/50 Hz AC needed by the motors of the pumps in the RO unit. The maximum input power and voltage of the inverter are 5.4 kW and 580 V, respectively; the maximum power point tracking voltage ranges from 125 to 550 V; and the rated output power is 4.6 kW.

### 2.7. Monitoring and control system

The system is monitored and controlled automatically. The data monitored are meteorological conditions including air temperature, solar irradiation and wind speed; electrical parameters including voltages, currents, and the state of the battery bank; and water parameters including pressures, flow rates, conductivity of permeate, seawater level in feed tank, and freshwater levels in product tank and cleaning tank. One PLC master module and three PLC extension modules are

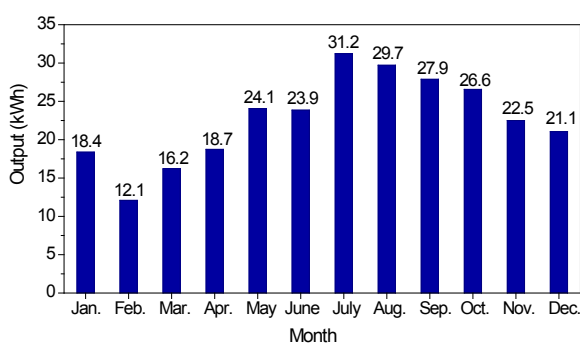


Fig. 3. Monthly electricity output of a selected single solar panel.

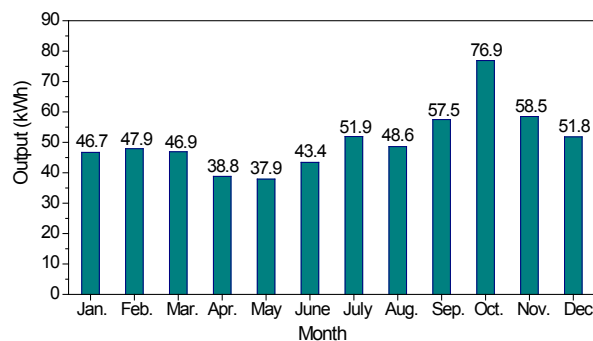


Fig. 4. Monthly electricity output of a single wind generator selected.

used to collect the analog signals from the measuring sensors and realize the automatic control of the system. The parameters are measured at an interval of 8 min, and screened and processed in a local computer. Through the Internet, the

operating conditions of the system can be monitored on any online computers. Figs. 7 and 8 give the photographs of the electric circuit and PLC modules as well as the touch-screen platform of the monitoring and control system.

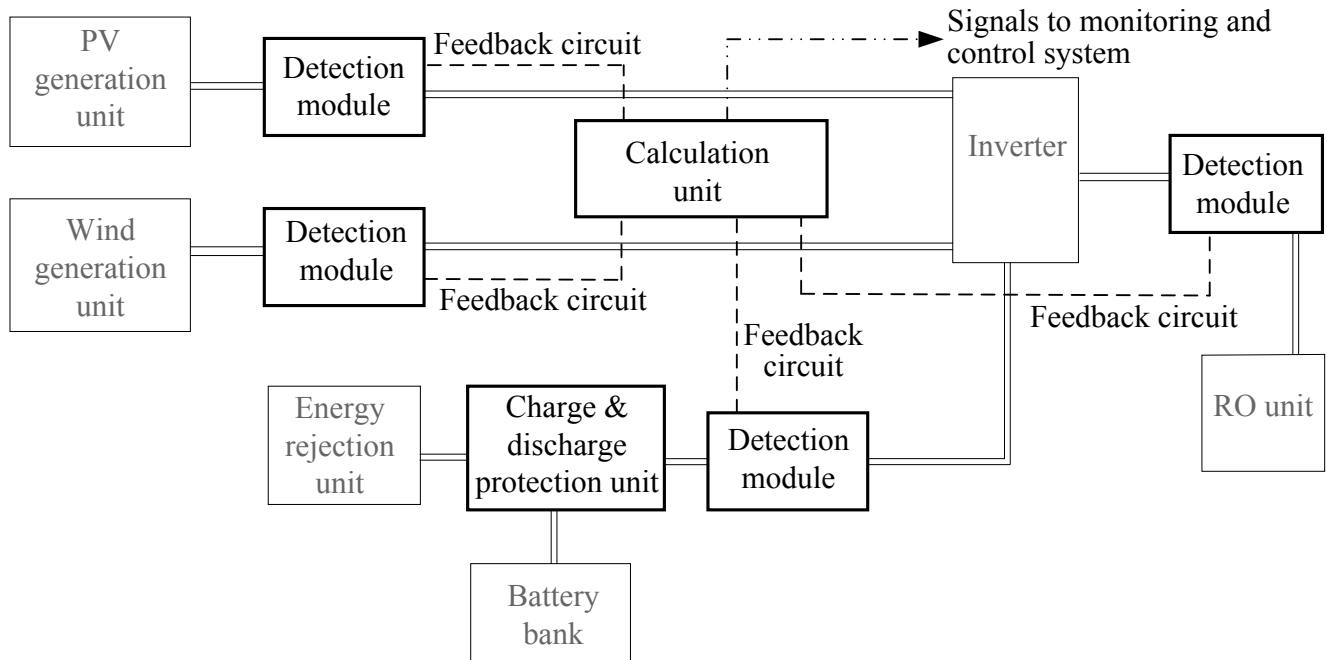


Fig. 5. Principle of the electricity equilibrium/buffer controller.

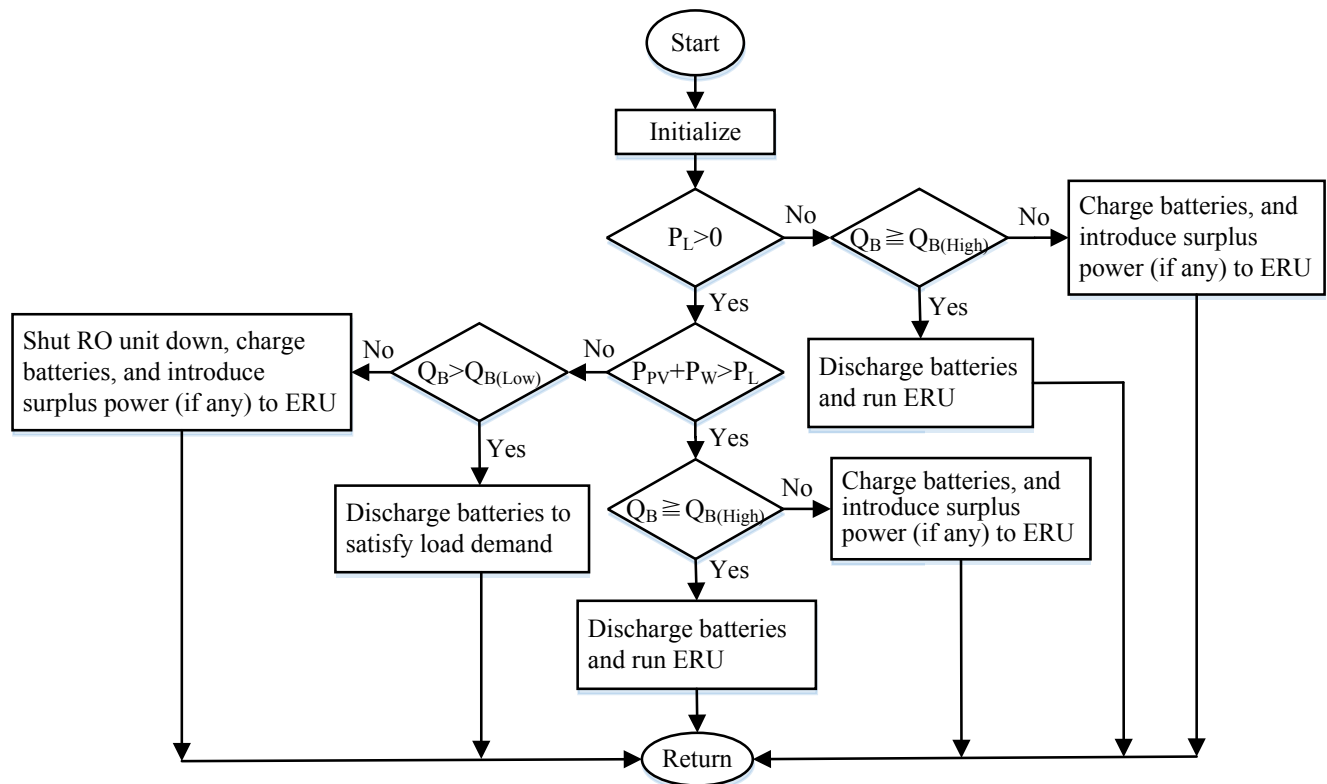


Fig. 6. Energy management strategy of the electricity equilibrium/buffer controller.

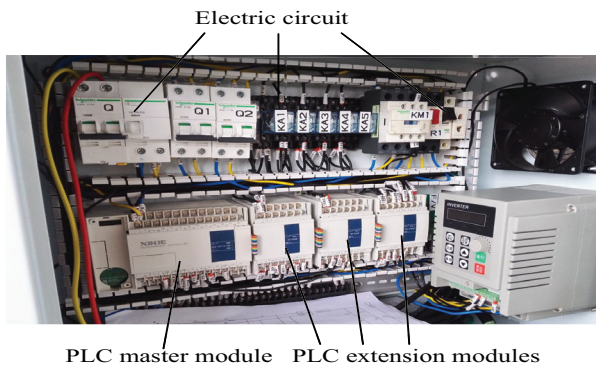


Fig. 7. Electric circuit and PLC modules for the monitoring and control system.



Fig. 8. Touch-screen monitoring and control platform.

Being monitored and managed 24 h/d, the experimental system can operate reliably in a full automatic mode. When the electricity produced by the solar and wind generators are monitored to be higher than 1.2 kW and the state of charge (SOC) of the battery bank higher than 40%, the RO unit begins to run. It is clear that the operation of the RO unit is possible only in the daytime because no enough energy is available to start it in the nighttime. The feed pump is started first, and after 3 min backward washing and 1 min forward washing of the multi-media filter, the feed is pretreated. When the feed pressure at the inlet of the high-pressure pump reaches 0.35 MPa, the high-pressure pump is started, gradually raising the feed pressure to a specified value. The produced permeate is fed to the cleaning tank in the first few minutes and then routed into the product tank. When the hybrid power and battery power cannot meet the load need, the RO unit will be shut down automatically, followed by the membrane cleaning process. In the case that the operating pressure is higher than the highest pressure allowed (5.5 MPa here), or the water level of the feed tank is too low, or the permeate salinity is higher than 1,000 ppm, the RO unit will be stopped immediately, with an alarm sounded.

### 3. Experimental results and discussion

The experiments of the hybrid PV-wind-powered desalination system were performed in an automatic mode

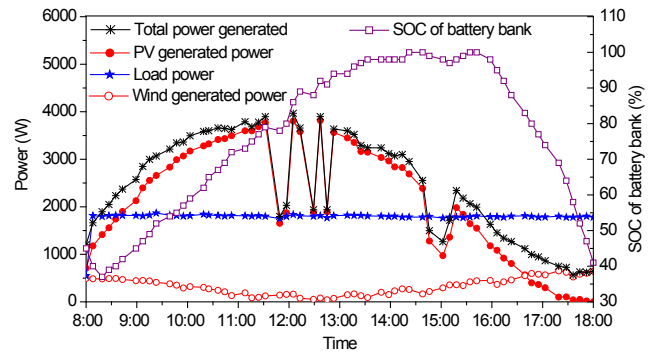


Fig. 9. Experimental results on September 11, 2015.

throughout September and October 2015. The operating pressure of the RO unit was set at 3.7 MPa, with corresponding power consumption of 1.75 kW and permeate flow rate about 150 L/h. As an example of the system performance, Fig. 9 gives the results obtained on September 11, during which the system ran for about 10 h, from 8:00 to 18:00, and about 1.5 m<sup>3</sup> of freshwater was produced. Real seawater with a salinity about 31,000 ppm was used as feed. The average salinity of the produced water was 231 ppm, indicating a salt retention rate of 99.2%.

It can be seen from Fig. 9 that the RO unit started to run at about 8:00 when both the hybrid power and the SOC of the battery bank reached the preset values, 1.2 kW and 40%, respectively. After several minutes' start-up process, the RO unit began to run steadily, with the consumed power kept almost constant, until it stopped running at about 18:00. Thanks to the battery bank, the system was able to run before 8:15 and after 15:50 when the hybrid power was inadequate, resulting in much longer operation time and then more water production than the corresponding non-battery system. Also thanks to the battery bank, the RO unit wasn't shut down but maintained a continuous operation from 14:42 to 15:02 when the hybrid power was lower than the load power. The SOC of the battery bank was 40% when the water production process stopped at about 18:00. Together with the wind power (if any), the battery bank was used to drive the high-pressure pump to perform membrane cleaning, and to maintain the operation of the monitoring/control system. Clearly, the small-capacity battery bank equipped played an important role in the stable and effective operation of the system.

The amount of electricity generated on September 11, 2015 was 25.3 kWh, 22.4 kWh by the PV array, and 2.9 kWh by the wind generators, while that consumed on the RO unit and the monitoring/control unit was 18.7 kWh, accounting for only 74% of the total amount. The balance (6.6 kWh, 26%) was lost mainly in the DC/AC inverting process occurred in the inverter, the charge and discharge processes of the battery bank, and the ERU. It was estimated that about 19% of the produced electricity had to be rejected through the ERU, which was obviously a great waste of energy. Calculation showed that appropriately changing the operating pressure and thereby the power consumption of the RO unit could help to reduce the amount of surplus electricity rejected. For example, simply regulating the operating pressure from 3.7 to 4.6 MPa, the rejected electricity would decrease from 19%

to 13%, and at the same time, the water production would increase by 17%.

Figs. 10 and 11 give the daily water and electricity production of the experimental system in September and October, respectively, and Table 3 gives a summary of the experimental results. The 2-month operation showed that the system was able to manage its energy and the operation of each component properly under unsteady solar and wind energies. Ran for 372 h (6.1 h/d averagely), the RO unit was start up and shut down almost every day, with the transmembrane flux remaining basically the same as that at the initial time. The intermittent off-and-on operation of the RO unit seems to have little influence on the membrane.

During the 2 months, the solar and wind generators generated 956 kWh of electricity, and the RO unit produced 55.8 m<sup>3</sup> of freshwater, resulting in a SPC of 17 kWh/m<sup>3</sup> of freshwater. The salinity of the produced water was kept below 300 ppm, much lower than the limit, 1,000 ppm, set by the Chinese government for drinking water [27]. Considering the feed salinity of 31,000 ppm, the salt retention rate was higher than 99%. The water recovery ratio was about 20%.

In the 956 kWh of generated electricity, 670 kWh was consumed by the RO unit, resulting in a net SPC of 12 kWh/m<sup>3</sup> for water production. This value is much higher than that of 2–5 kWh/m<sup>3</sup> [28] of the commercialized RO units, for which the main reason is that considering the small capacity of the experimental system, no energy recovery device was equipped for simplicity. Calculations showed that the net SPC would decrease by 50% by adding a pressure energy recovery device to the RO unit. Based on the total electricity produced, the gross SPC was 17 kWh/m<sup>3</sup>, 42% higher than the net SPC. As mentioned before, the difference was mainly caused by the energy loss in the inverter, the battery bank, and the ERU. It was estimated that the energy rejected in ERU accounted for more than 20% of the total electricity generated. To utilize the produced electricity more efficiently, we are now doing calculations based on the climatic conditions of Xiamen to try to obtain the yearly or seasonally optimal operating pressure of RO.

During the 2-month operation, 837 kWh of electricity was generated by the PV array, 23% less than expected (based on Fig. 3, the output was expected to be 1,090 kWh), and 119 kWh by the wind generators, 56% less than expected (based on Fig. 4, the output was expected to be 269 kWh). Clearly, solar power played a more important role in practice than designed. In the 956 kWh of generated electricity, 87.5% was from the solar array, and only 12.5% from the wind generators. Limited by the on-site conditions, the solar panels and wind turbines were installed on the fifth-storey rooftop of a building, which had six storeys in the middle and five storeys on both sides. The resistance of the pitched roof and the walls of the sixth-storey rooms lowered the wind speed and then the wind power output. The solar panels were supported about 3 m high by metal supports, partly reduced the influence of the shade of the roof and walls on solar power production. With an average output of only 2 kWh/d, the wind generators had quite limited contribution to water production in our experiments, but mainly helped to maintain the running of the monitoring/control system at nights and on rainy and cloudy days.

It is reflected in Figs. 10 and 11 that higher electricity production generally leads to higher water production,

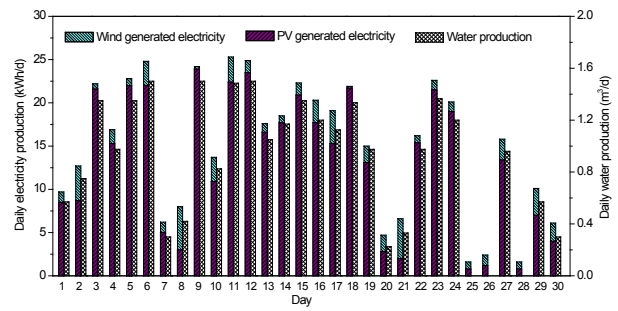


Fig. 10. Daily water and electricity production in September 2015.

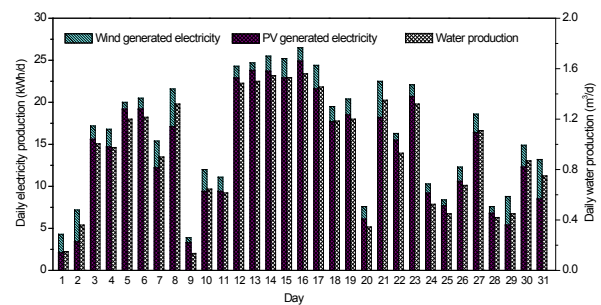


Fig. 11. Daily water and electricity production in October 2015.

Table 3  
Summary of experimental results in September and October 2015

	Total	Daily maximum	Daily minimum	Daily average
Solar power production, kWh	837	24.9	0.8	13.7
Wind power production, kWh	119	4.7	0.2	2
Hybrid power production, kWh	956	26.5	1.6	15.7
Operation time of RO unit, h	372	10.4	0	6.1
Water production, m <sup>3</sup>	55.83	1.56	0	0.92

but the relation is not strictly monotonic. For example, 24.2 and 24.4 kWh of electricity was generated on September 9 and October 17, while 1.5 m<sup>3</sup> and 1.45 m<sup>3</sup> of water was produced, respectively, indicating that more electricity was lost in ERU on October 17. Generally speaking, as the dominant driving source, higher solar-generated electricity is expected to lead to higher water production, which is also reflected in Figs. 9 and 10, with the relation also not strictly monotonic.

The daily average water production was 0.92 m<sup>3</sup>/d, close to the design capacity of 1 m<sup>3</sup>/d. The maximum amount of water, 1.56 m<sup>3</sup>, was produced on October 16, while no water

was produced on September 25, 26, and 28, implying the necessity of water storage. It can be seen from Table 2 and Fig. 3 that the solar insolation in July and August is higher than that in September and October, indicating more solar power output and then more water production in July and August, say, near or over 1 m<sup>3</sup>/d. The solar insolation in other months, especially in the first 4 months of the year, is much lower and is expected to have lower water production. Taking 1 year as a period, the water production of the experimental system would be lower than designed, for which the main reasons are two: reduced electricity production caused by the limitation of experimental site and low-efficiency utilization of the produced electricity.

Solar energy and wind energy are considered to be mutually complementary. This point was not fully reflected in our experiments, mainly because that: (1) with a yearly average wind speed of 3 m/s, Xiamen is not rich in wind resource, and (2) limited by the on-site conditions, the wind energy was not utilized effectively. Nevertheless, we got a lot of experience of designing and operating a hybrid solar-wind-powered RO desalination system, which is greatly helpful for us to develop the demonstration system that will be built before long on the Tuyu Island, a wind-rich island 1.6 km away from the coast of Xiamen.

#### 4. Conclusions

Based on the experimental setup developed, experiments were carried out on the hybrid PV-wind-powered desalination system, with the results reported and discussed in this paper.

The system ran automatically throughout September and October 2015, showing good suitability to unsteady solar and wind energies, during which the RO unit ran for 372 h (6.1 h/d on the average), showing reliable performance in the intermittent off-and-on operation mode. The specially designed electricity equilibrium/buffer controller managed the produced, demanded, stored, and rejected power properly, and the monitoring/control system ensured a real-time monitoring and fully automatic control of the experimental system. Partly getting rid of the disadvantages of large battery banks, the small-capacity battery bank with only 1.5-h storage autonomy used in the system was greatly helpful in maintaining a stable power for water production.

During the 2-month operation, real seawater with a salinity of 31,000 ppm was used as feed, and the produced permeate kept a salinity lower than 300 ppm, resulting in a salt retention rate higher than 99%. The daily water production was in the range of 0–1.56 m<sup>3</sup>/d, and the average was 0.92 m<sup>3</sup>/d. The SPC of freshwater was 17 kWh/m<sup>3</sup>. More attention should be paid on optimizing the operating pressure of the RO unit and thus making the demanded power more matchable to the produced power to reduce the amount of energy discarded through the ERU.

#### Acknowledgments

The authors gratefully acknowledge the support of the National Natural Science Foundation of China (Project No. 51676085), the Xiamen Southern Ocean Research Center,

China (Project No. 14GZB64NF28), and the Educational Department of Fujian Province, China (Project Nos. JA15258 and JAT160264).

#### Symbols

P	—	Power, kW
Q	—	Charge capacity of battery bank, kWh

#### Abbreviations and subscripts

AC	—	Alternative current
B	—	Battery bank
ch	—	Charge
DC	—	Direct current
dch	—	Discharge
ERU	—	Energy rejection unit
L	—	Load
PV	—	Photovoltaic
RO	—	Reverse osmosis
SOC	—	State of charge
SPC	—	Specific power consumption
TDS	—	Total dissolved solid
W	—	Wind

#### References

- [1] <http://idadesal.org/desalination-101/desalination-by-the-numbers/> (Accessed on 05.12.16).
- [2] D. Xevgenos, K. Moustakas, D. Malamis, M. Loizidou, An overview on desalination and sustainability: renewable energy-driven desalination and brine management, *Desal. Wat. Treat.*, 57 (2016) 2304–2314.
- [3] A. Cipollina, E. Tzen, V. Subiela, M. Papapetrou, J. Koschikowski, R. Schwantes, M. Wiegand, G. Zaragoza, Renewable energy desalination: performance analysis and operating data of existing RES-desalination plants, *Desal. Wat. Treat.*, 55 (2015) 3120–3140.
- [4] A. Mahesh, K.S. Sandhu, Hybrid wind/photovoltaic energy system developments: critical review and findings, *Renew. Sustain. Energy Rev.*, 52 (2015) 1135–1147.
- [5] E. Tzen, M. Sigalas, Clear water: development of an autonomous PV wind hybrid desalination system, *Refocus*, 5 (2004) 30–31.
- [6] E. Koutroulis, D. Kolokotsa, Design optimization of desalination systems power-supplied by PV and W/G energy sources, *Desalination*, 258 (2010) 171–181.
- [7] E.S. Mohamed, G. Papadakis, Design, simulation and economic analysis of a stand-alone reverse osmosis desalination unit powered by wind turbines and photovoltaics, *Desalination*, 164 (2004) 87–97.
- [8] H. Cherif, J. Belhadj, Large-scale time evaluation for energy estimation of stand-alone hybrid photovoltaic-wind system feeding a reverse osmosis desalination unit, *Energy*, 36 (2011) 6058–6067.
- [9] E.M.A. Mokheimer, A.Z. Sahin, A. Al-Sharafi, A.I. Ali, Modeling and optimization of hybrid wind-solar-powered reverse osmosis water desalination system in Saudi Arabia, *Energy Convers. Manage.*, 75 (2013) 86–97.
- [10] K. Mousa, A. Diabat, H. Fath, Optimal design of a hybrid solar-wind power to drive a small-size reverse osmosis desalination plant, *Desal. Wat. Treat.*, 51 (2013) 3417–3427.
- [11] S.A. Kershman, J. Rheinländer, T. Neumann, O. Goebel, Hybrid wind/PV and conventional power for desalination in Libya—GECOL's facility for medium and small scale research at Ras Ejder, *Desalination*, 183 (2005) 1–12.
- [12] I.D. Spyrou, J.S. Anagnostopoulos, Design study of a stand-alone desalination system powered by renewable energy sources and a pumped storage unit, *Desalination*, 257 (2010) 137–149.

- [13] A.A. Malki, M.A. Amri, H.A. Jabri, Experimental study of using renewable energy in the rural areas of Oman, *Renew. Energy*, 14 (1998) 319–324.
- [14] D. Weiner, D. Fisher, E.J. Moses, B. Katz, G. Meron, Operation experience of a solar- and wind-powered desalination plant, *Desalination*, 137 (2001) 7–13.
- [15] Y. Deng, Application Research on Reverse Osmosis Seawater Desalination System Driven by Hybrid Wind-Solar Energy, Master's Thesis, Shantou University, China, 2011 (in Chinese).
- [16] B. Feng, Z. Zhang, Seawater desalination system powered by wind and solar hybrid micro-grid, *Renew. Energy Resour.*, 33 (2015) 1281–1286 (in Chinese).
- [17] X. He, S. Yang, K. Wang, X. Zhang, J. Xu, X. Zhang, The development of a small-scale wind-solar powered reverse osmosis desalination unit, *Water Treat. Technol.*, 38 (2012) 92–94 (in Chinese).
- [18] S. Yang, China Seawater Desalination Yearbook 2010, China Ocean Press, Beijing, 2012 (in Chinese).
- [19] <http://www.filmtecmembranes.com> (Accessed on 05.12.16).
- [20] [http://www.xm.gov.cn/zjxm/xmgk/200708/t20070830\\_173889.htm](http://www.xm.gov.cn/zjxm/xmgk/200708/t20070830_173889.htm) (Accessed on 05.12.16).
- [21] D. Song, Climates of Fujian islands, China Meteorological Press, Beijing, 1996 (in Chinese).
- [22] Climatic Data Center of China Meteorological Administration and Department of Building Science and Technology in Tsinghua University, Meteorological Data Set for Thermal Environment Analysis of Buildings in China, China Architecture & Building Press, Beijing, 2005 (in Chinese).
- [23] J. Liu, B. Yu, Y. Jiang, Wind energy potential assessment of Fujian Province in China, *Renew. Energy Resour.*, 25 (2007) 59–61 (in Chinese).
- [24] Z. Wu, Z. Ye, H. Shen, Application of New Energy and Renewable Energy, Mechanical Industry Press, Beijing, 2006 (in Chinese).
- [25] E.S. Mohamed, G. Papadakis, E. Mathioulakis, V. Belessiotis, An experimental comparative study of the technical and economic performance of a small reverse osmosis desalination system equipped with a hydraulic energy recovery unit, *Desalination*, 194 (2006) 239–250.
- [26] M. Thomson, D. Infield, A photovoltaic-powered seawater reverse-osmosis system without batteries, *Desalination*, 153 (2003) 1–8.
- [27] Ministry of Health of China and Standardization Administration of China, Standard for Drinking Water Quality, GB 5749-2006 (in Chinese).
- [28] S.S. Shenvi, A.M. Isloor, A.F. Ismail, A review on RO membrane technology: development and challenges, *Desalination*, 368 (2015) 10–26.